Suspension system design for a vehicle under BAJA SAE parameters

Omar Franco-Camacho *,[a], María Mago-Ramos [a], Ricardo Ríos [a], Luis Vallés-Defendine [b]

[a]*Maintenance Research Line, Faculty of Engineering, Universidad Libre, Mechanics Program, Bogota, Colombia.*
[b]*Faculty of Engineering, Universidad de Carabobo, Mechanics Program, Valencia, Venezuela.*

Abstract.- This research focuses his study on the design of a suspension system for a BAJA SAE vehicle under the PARAMETERS SAE (Society of Automotive Engineers). This society organizes seventeen (17) student competitions in eight (8) design series between university students called as Collegiate Design Competitions and Collegiate Design Contests, which is included representative themes that apply to vehicles Formula SAE, Formula Hybrid, SAE Aero Design, BAJA SAE, and SAE Clean Snowmobile Challenge. This research article evaluates the types of suspension that are implemented in mini-baja vehicles, and which, in turn, complies with the regulations established by the SAE competition of the year 2020. The methodology used from the mechanical engineering and control design components, use mathematical equations that govern dynamic movement to evaluate the behavior of the suspension system that through a CAD system, achieves modeling in a real environment, evaluating factors such as material, part dimensions or system selection, which can affect its proper functioning. This research is intended to support future applications, where there are suspension systems that allow to absorb the irregularities of the terrain with loads, where it is transmitted in less proportion according to the structure of the vehicle improving the experience of handling and maneuverability required for this type of student competitions, meeting the parameters established by SAE.

Keywords: design; suspension system; mini-baja vehicle; SAE parameters.

Diseño del sistema de suspensión para vehículo de acuerdo con parámetros BAJA SAE

Resumen.- Esta investigación centra su estudio en el diseño de un sistema de suspensión para un vehículo BAJA SAE bajo los Parámetros SAE (Sociedad de Ingenieros Automotrices). Esta sociedad organiza diecisiete (17) concursos de estudiantes en ocho (8) series de diseño entre estudiantes universitarios denominados Competencias de Diseño Colegiado y Concursos de Diseño Colegiado, que incluyen temas representativos que se aplican a los vehículos Fórmula SAE, Fórmula Híbrida, SAE Aero Diseño, BAJA SAE, y SAE Clean Snowmobile Challenge. Este artículo de investigación evalúa los tipos de suspensión que se implementan en los vehículos mini-baja, y que, a su vez, cumplen con la normativa establecida por el concurso SAE del año 2020. La metodología utilizada a partir de los componentes de ingeniería mecánica y diseño de control, utiliza ecuaciones matemáticas que gobiernan el movimiento dinámico para evaluar el comportamiento del sistema de suspensión que a través de un sistema CAD, logra el modelado en un entorno real, evaluando factores como material, dimensiones de la pieza o selección del sistema, que pueden afectar su correcto funcionamiento. Esta investigación tiene como objetivo dar soporte a futuras aplicaciones, donde existan sistemas de suspensión que permitan absorber las irregularidades del terreno con cargas, donde se transmita en menor proporción según la estructura del vehículo mejorando la experiencia de manejo y maniobrabilidad requerida para ello, mejorando las competencias de los estudiantes, cumpliendo los parámetros establecidos por la SAE.

Palabras clave: diseño; sistema de suspensión; vehículo Mini Baja; parámetros SAE.

Received: October 28, 2020.
Accepted: November 27, 2020.

1. Introduction

The manufacture of BAJA SAE vehicles today is carried out in different universities as a degree option, in order to compete in the SAE Design Series® under different modalities, where it is innovated from mechanical engineering

* Correspondence author:
*e-mail:*omara-francoc@unilibre.edu.co (O. Franco-Camacho)

exchanging knowledge and experiences to expand the professional vision of the student.

In this order of ideas, this research adjusts its contribution in the line of maintenance research, supporting the processes and competencies that the student of the Mechanical Engineering Program of the Free University can develop for the sectors of the automotive area, in terms of design applications of these baja SAE vehicles is concerned, deepening knowledge and applications in a practical way. Likewise, a mathematical analysis is used in the modeling of the parts that constitute said automobile, its correct simulation provides information to the student and/or technical staff interested in these areas of knowledge, of an optimal performance that manages to adapt the vehicle to the regulations of the competition for the year 2020 and obtaining the control and safety required, which will allow to occupy a relevant position in this type of competitions [1, 2].

Based on the above, this research is expected to show the design parameters required by the suspension system of the V1.0 BAJA SAE vehicle, under the expertise of the mechanical engineering student, in order to achieve a reduction in the weight of the suspension system and decrease the efforts caused by the loads in the supports generated by the irregularities of the terrain, as well as a linkage of the theoretical components and applications required by the automotive sectors in real way [3, 4].

2. Methodology

For the elaboration of the required suspension system, it was chosen to perform a simulation with ANSYS, for a correct selection of the latter, taking into account the critical variables to analyze, in addition, Matlab's Simulink was used to obtain a dynamic behavior of the vibrations produced by the ground, through a graphical programming environment to model, simulate and analyze dynamic systems that have multidomain [5, 6, 7]. This research features simulated analysis of failures and behaviors in controlled environments, by implementing these software programs better performance in real applications such as the SAE competition. The suspension system models are correlated in such a way that a dynamic model is simulated according to irregularities of the terrain through an analysis of the stationary system and its calculated maximum load, where the manufacturer's data that has been selected in the design proposal is corroborated and then make design improvements adapted to the market [8, 9].

2.1. Compression spring or springs

This research makes use of a series of springs that follow the shock to withstand the stresses produced by the irregularities of the terrain, providing greater stability, passenger comfort, aid to the recoil of the shock at the time of the shock, decreasing the pressure exerted in this, so a coil spring of compression is used (The helical spring is the most widely used on the market nationally in Colombia for general use in valves, greasers and shock absorbers) [10]. There are cylindric, conical, bionic and stamping coil compression springs, however, a cylindrical helical spring will be used, as this represents better attributes because it withstands lower tension than the other types of springs, so it distributes the loads evenly throughout it [11, 12, 13].

2.2. Spring materials

The springs are manufactured by cold or hot procedures, depending on the size of the material, the spring index and the desired properties, often during the manufacture of springs, they are relieved, after rolling, by means of moderate heat treatment according Table 1.

A compression helical spring with an original free length closes completely and returns to a reduced value. The process of inducing a permanent deformation is used by spring manufacturers to meet a free length specification or to reinforce the spring, this process is called L_o "deformation removal" [15, 16].

In that order of ideas, a coil spring used in the suspension of the mini-baja vehicle has elastic properties and good toughness, to absorb the shock between the surface and the chassis of the vehicle, for this reason, materials such as 6150 H tempered

Table 1: Carbon and spring alloy steels [14]

Piano Wire, 0.80-0.95C	UNS G10850	The most tenacious and employed
	AISI 1085	Increased stress resistance
	ASTM A228-51	Increased efforts at repeated loads
		Diameters from 0,12 to 3 mm
Oil-hardened wire, 0.60-0.70C	UNG G10650	It is for general use
	AISI 1065	It's cheaper than piano wire
	ASTM 229-41	Not suitable for shock or impact loads
		Diameters from 3 to 12 mm
Hard drawn wire, 0.60-0.70C	UNS G 10660	General and cheaper use
	AISI 1066	It should only be used where duration, accuracy and deflection are not important
	ASTM A227-47	Diameters 0.8 to 12 mm
Chromium vanadium	UNS G61500	Popular alloy for springs that involve greater stresses than those that employ carbon steel and requires fatigue resistance and high durability.
	AISI 6150	Used for shock or impact loads
	ASTM 231-41	Diameters 0.8 to 12 mm
Silicon chromium	UNS G92540	It is an excellent material alloy for springs subjected to high stresses and impact loads that require long life
	AISI 9254	Diameters 0.8 to 12 mm

steel trefiled wires, cooleds in oil, annelids, with a diameter of 9 mm [17, 18, 19].

2.3. *Helical spring design*

Due to the value of the equipment required by the suspension systems, the properties of the materials, the necessary parametric relationships, their adequacy assessment in terms of weight reduction, increase of the safety factor and design, which is necessary to take into account the maximum stresses, curvature effects, deflection-force ratios, tensile and compression efforts, as indicated in the following equations.

Where; the maximum stress of the wire is calculated by overlaying equations (equation (1)).

$$\tau_{\text{máx}} = \pm\frac{T_r}{J} + \frac{F}{A} \tag{1}$$

$\tau_{\text{máx}} = \dfrac{T \cdot \rho}{J}$. It is the formula of the maximum torque (in order to calculate the particular effort).

$\dfrac{F}{A}$: is direct shear stress (not bending).

But it is necessary to calculate the spring index as follows in equation (2), and the constant stress factor in equation (3).

$$C = \frac{D}{d} \tag{2}$$

$$K_s = \frac{2C+1}{2C} \tag{3}$$

Torque may be measured by a measure of the spiral curvature (which also determines the larger shear stress), as indicated in equation (4).

$$\tau = K_s = \frac{8FD}{\pi D^3} \tag{4}$$

In addition, the curvature correction factor increases the stress inside the spring, but only decreases a little on the outside, which is important for fatigue, even if there is no stress concentration factor as indicated in equation (5).

$$K_C = \frac{K_B}{K_S} = \frac{2C(4C+2)}{(4C-3)(2C+1)} \tag{5}$$

The deflections of coil springs have a deflection-force ratio obtained by the Castigliano theorem, where the total corresponding deformation energy is shown in equation (6).

$$U = \frac{T^2}{2GJ} + \frac{F^2 l}{2AG} \tag{6}$$

$$y = \frac{\partial U}{\partial F} = \frac{8FD^3}{d^4 G}\left(1 + \frac{1}{2C^2}\right) \approx \frac{8FD^3 N}{d^4 G}$$

where the spring ratio is therefore;

$$k = \frac{d^4 G}{8D^3 N} \tag{7}$$

Extension springs must have means to transfer the load from the spring to the spring body, the stress increase factors are given by equation (8), as indicated (The C index is in Table 1).

$$(K)_A = \frac{4C^2 - C_1 - 1}{4C_1(C_1 - 1)}; C_1 = \frac{2r_1}{d} \tag{8}$$

Table 2: Preferred range of torsional stresses due to initial stress, in steel extension coil springs [20]

Index (C)	Stress Interval (MPa)	Stress interval (kpsi)
4	115-183	16,7-26,6
6	95-160	13,8-23,2
8	82-127	11,9-18,4
10	60-106	8,71-15,4
12	48-86	6,97-12,5
14	37-60	5,37-8,71
16	25-50	3,63-7,26

Compression springs have four types of ends: simple type on the right, end to square and frosted on the left, end-to-square or closed right and simple end and frosted on the left, being necessary for the calculation of the dimensions of these springs review Table 3.

2.4. *Stability*

A column will suffer buckling when the load is very high, so the coil springs will have a lateral deflection (roll) when it is very large, taking into account that the critical deflection is given by equation (9).

$$y_{cr} = L_o C_1' \left[1 - \left(1 - \frac{C_2'}{\lambda_{\text{efec}}^2} \right)^{\frac{1}{2}} \right] \tag{9}$$

Where;
y_{cr}:deflection corresponding to the onset of instability.
λ_{efec}: effective slenderness ratio.
C_1' y C_2': elastic constants.
L_o: absolute stability.

2.5. *Description of the structure*

The structure used in this research is a shock absorber whose spring is SAE 6150 H steel (Figure 1) with the addition of vanadium that allows to inhibit the growth of the grain at high temperatures, improve the strength and toughness of the spring, in order to have high degrees of elasticity (Table 3), also, the 6150 H steel has the material components indicated in Table 4 and 5. This suspension system has the dimensions required for the perfect coupling to the vehicle [21, 22, 23].

3. CAD modeling and simulation for dynamic analysis

For the analysis of behavior of static suspension system as shown in Figure 1, the shock absorber subjected to a load was modeled and simulated with the ANSYS software. On the other hand, for the analysis of structure dynamic behavior, the system was modeled and simulated with ANSYS, SolidWorks and Matlab. All these software apply the finite element analysis technique to predict how the system will work and react in a real environment, allowing to evaluate the performance of the system before the manufacturing process. Now, the mathematical model for static analysis follows equation (10) [24, 25].

$$\varepsilon = \frac{\Delta L}{L} = \frac{F}{AE} \tag{10}$$

Where it is evident, that the unitary elongation experienced by the spring is directly proportional to the force applied on it. Using for this case the mathematical model shown in equation (11) of the Law of *Hooke*, which relates the force exerted by the spring to the elongation (x) provoked by the external force (F) applied to the end of this, as follows according to (11).

$$F = -k \cdot x \tag{11}$$

The suspension has its critical point at the time the vehicle jumps and its weight falls on both wheels, so a dynamic analysis is performed with a 45-degree lifting angle as seen in Figure 2.

Table 3: Formulas for calculating compression spring dimensions [20]

Term	Simple	Simple and frosted	Squared and closed	Squad and frosted
Extreme coils	0	1	2	2
Total spire	N_{to}	N_{to} + 1	N_{to} + 2	N_{to} + 2
Free length	$p \cdot N_{to} + d$	$p \cdot N_{to} + 1$	$p \cdot N_{to} + 3d$	$p \cdot N_{to} + 2d$
Solid length	$d(N_1 + 1)$	dN_1	$d(N_1 + 1)$	dN_1
Step	$(L_o - d)/N_a$	$L_o/(N_{to} + 1)$	$(L_o - 3d)/N_{to}$	$(L_o - 2d)/N_a$

Figure 1: JLMoto brand suspension system dimensioning reference 3100026.
Source: Jl motor official store, https://bit.ly/3p66Gxi

Table 4: Steel elements SAE 6150 H

Element	Content %
Iron, faith	96,885 – 97,88
Manganese, Mn	0,60 – 1
Chromium, Cr	0,75 – 1,2
Silicon, Yes	0,15 – 0,30
Vanadio, V	0,15
Sulfur, S	0,040
Phosphorus, P	0,035

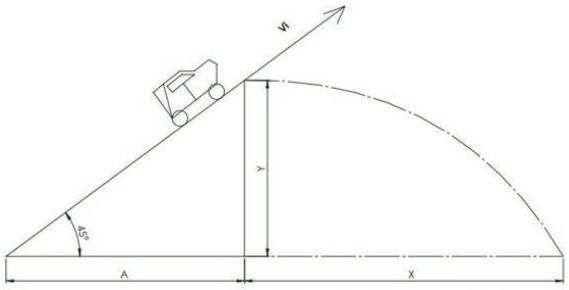

Figure 2: Critical load model scheme

Table 5: Good properties of steel SAE 6150 H

Property	International System
Tensile strength	924 MPa
Elastic limit	800 MPa
Elasticity module	205 GPa
Volume module	140 GPa
Cutting module	80 GPa
Poisson coefficient	0,29
Elongation to breakage	19,50 %
Brinell hardness	269
Rockwell B hardness	99
Rockwell C hardness	27
Machinability	55 %

The speed at which the vehicle hits the ground in a given flight time is then calculated.

In that sense, accordigng the model presented in Figure 2, the followings characteristic parameters can be estimated.

The Final speed is calculated by equation (12).

$$V_f = V_i \cos 45(i) + V_i \sin 45 - gt(j) \qquad (12)$$

when: g: gravity, [m/s^2]
t: time, [s].
V_i: initial velocity, [m/s]. V_i= 13,88 m/s
$\tan 45°$: Y/A
y: vertical component, [m].

A: horizontal component, [m].
Distance A-1 m.

The Horizontal distance reached, knows as X value (m), was calculated by equation (13).

$$Y = \frac{(\tan 45°)X - (gX^2)}{2V_i 2\cos(45°) + 1} \tag{13}$$

By developing the quadratic equation, you get:

$$1 = X - 0.050X^2$$
$$0.050X^2 - X + 1 = 0$$
$$X_1 = 2\ m; X_2 = 18\ m$$

Where X^2 is the distance taken for the following calculations, because it is the vertical component.

To determine the Flight time it was used equation (14).

$$t = \frac{x}{V_i \cos 45°} \tag{14}$$

It is necessary to know and work with the vertical component, as it corresponds to the force with which the vehicle will exert a compression load on the suspension system.

Final velocity component Y $[m/s]$ was estimated by equation (15), as follows.

$$V_{f_y} = (V_i \sin 45° - gt)\, j \tag{15}$$

At the same time, the Average strength $[N]$ was calculated by equation (16), as fallows.

$$F_{\text{prom}} = \frac{\Delta p}{\Delta t} \tag{16}$$

$$\Delta p = mV_f - mV_i$$

Δt: time delta [s]. $\Delta t = 0.5$ s

To Suspension system calculations, it was considered m = 265 kg with approximately 70 kg rider. In that sense, taking as start point equation (17), the force can be calculated.

$$F = m \cdot a \tag{17}$$

a: Acceleration, [m/s^2].
m: mass of a rider, [kg].

$$F = 265\ kg \cdot 9,81\ \text{m/s}^2 = 2599,65\ \text{N}$$

Spring calculations are based in equation (18).

$$F = kx \tag{18}$$

k: spring constant, [kg/s^2].
x: variation in length, [m].

$$k = \frac{2599,65\ \text{N}}{0,05\ \text{m}} = 51993\ \text{kg/s}^2$$

According to the manufacturer's data, the spring distance is 207 mm and the distance of the compressed spring is 70 mm

$$F = 51993\ \text{kg/s}^2 \cdot 0,137 = 7123,041\ \text{N}$$

In this way, you have a compression coil spring made of Chromium-vanadium number 17, whose outer diameter is inches and the ends are flat and frosted $\frac{7}{16}$ inches with a total turn $10\frac{1}{2}$.

To estimate Creep effort are used equations (19) and (20).

$$s_{ut} = \frac{A}{d^m} = \frac{169}{0.039^0.168} = 291\ \text{kpsi} \tag{19}$$

$$s_{sy} = 0.45 \cdot s_{ut} = 0.45(291) = 131\text{kpsi} \tag{20}$$

To determine the static load according to creep effort, it is considered that the medium diameter of the spring coil is $\frac{7}{16} = 0,400$ inches. So, parameters C, K_B and F are calculated by equations (21), (22) y (23)

$$C = \frac{0,400}{0,039} = 10,3 \tag{21}$$

$$K_B = \frac{4C + 2}{4C - 3} = 1,131 \tag{22}$$

$$F = \frac{\pi d^3 s_{sy}}{8K_B D} = \frac{\pi(0,039)^3 \cdot 131(10^3)}{8(1,131) \cdot 0,400} \tag{23}$$
$$F = 6,75\ lbf$$

where
C: Spring index, [m].
K_B: Bergstrosser's factor.
F: Cutting force, [lbf].

To determine the spring scale is used equation (8), obtaining k factor

$$k = \frac{d^4 G}{8D^3 N_a} = \frac{(0,039)^4 (11.2)10^6}{8(0,400)^3 (9,5)}$$

$$k = 5,33 \text{ lbf/pulg}$$

In that sense, deflection caused by shear force is calculated by equation (24)

$$y = \frac{F}{k} = \frac{6,75 \text{ lbf}}{5,33 \text{ lbf/pulg}} = 1,26 \text{ pulg} \qquad (24)$$

So, the solid spring length is estimated by equation (25)

$$L_s = d \cdot N_t \qquad (25)$$

$$L_s = (0.039)(10.5)$$

$$L_s = 0.400 \text{ pulg}$$

Equations (26) allows to estimate the free length (L_o) as follows

$$L_o = y + L_s = 1,26 + 0,400 = 1,66 \text{ pulg} \qquad (26)$$

L_o: [pulg] .

To verify the absolute stability to prevent buckling, it is necessary the accomplish of condition:

$$L_o \leq 2,63\frac{D}{\alpha} \leq 2,63\frac{0,400}{0,5} \leq 2,10 \text{ pulg}$$

Because the free length is less than 2,10 inches; a buckling in the spring may not occur, however, a rod inside it may be necessary, resulting in the use of the shock as a mechanical aid component in the system [26, 27].

Finally, the step between coils is calculated by equation(27)

$$p = \frac{L_o}{N_a + 1} = \frac{1,66}{9,5 + 1} = 0,158 \text{ pulg} \qquad (27)$$

In the Table 6 is presented a resume of the parameters estimated by the aplication of the models mentioned.

Table 6: Results given after the application of the models

Horizontal distance reached, [m]	$X_1 = 2$ $X_2 = 18$
Flight Time (t), [s]	1,83
Final velocity component Y (Vf_y), [m/s]	-8,14
Average strength ($FpromY$), [N]	4314,2
Spring force (F), [N]	2599,65
Spring constant (k), [kg/s^2]	51993
Hooke's law (F), [N]	7123,041
Static load force (F), [N]	30,0255
Spring scale (k), [N/m]	933,46
Deflection (y), [m]	0,032
Solid spring length (L_s), [m]	0,010
Free length (L_o), [m]	0,053

4. Simulation for shock analysis

In accordance with the design of the suspension system previously performed, a simulation is carried out using the Matlab Simulink Program, in order to observe the behavior under established parameters, thus the expected result is to reduce costs and time in the manufacture of these systems in the automotive industry. The results obtained are of interest, when evaluating the time of restoration of the system from the starting point and the on peaks that can reach when generating the crash, with the irregularities of the terrain, based on free models [1].

The above makes it necessary to raise the system state equations, having as a parameter the acceleration a time range. As the system is purely mechanical, it does not have an electrical part, so Newton's second law is used to determine the model of the state equation as noted below (Figure 3) [28, 29].

$$\sum F_i = F_t$$

$$m\ddot{x} + k[x - y] + c[\dot{x} - \dot{y}] = 0$$

$$m\ddot{x} = k[y - x] + c[\dot{y} - \dot{x}] = 0$$

$$\ddot{x} = \frac{1}{m}[k[y - x] + c[\dot{y} - \dot{x}]]$$

where:

$\ddot{x}$: acceleration of the system, [m/s^2].

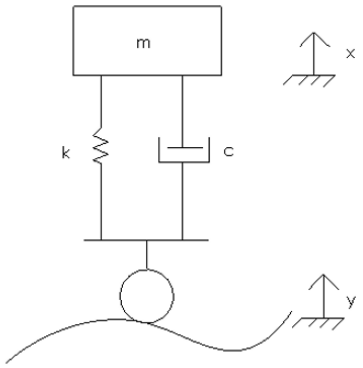

Figure 3: free body diagram of suspension system

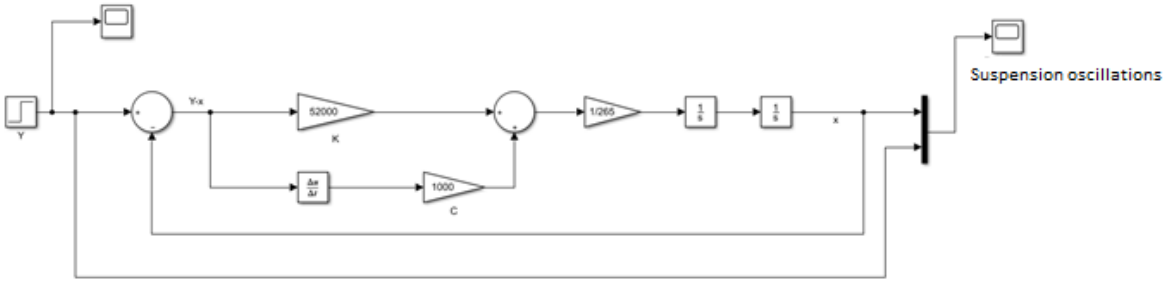

Figure 4: Control model for dynamic study of the suspension system

$\dot{x}$: speed of the system, [m/s].
x: system displacement, [m].
$\dot{y}$: wheel speed, [m/s].
y: wheel displacement, [m].
m: mass, [kg]. $m = 256$ kg
k: spring constant, [N/m]. $k = 52000$ N/m
c: Viscous coefficient of friction, [N·s/m]. $c = 1000$ N · s/m

The Figure 4 shows the diagram of the implemented control and how it shows the oscillation of vibrations in the system over time. Obtaining from the previous model, a peak envelope of three (03) centimeters of deformation when taking a system input disturbance of two (02) centimeters as the initial value to which you want to reach, once the suspension, into contact with their regularities of the terrain. It is also observed that the system has a one-second signal start time as part of the system behavior with a stabilization time of approximately four seconds until the required control signal is reached (Figures 4 and 5).

It can be verified that the suspension system properly absorbs the irregularities of the terrain in a time of 4 seconds to maintain stability and comfort in the driver. Likewise, you can control the number of oscillations that this can have by varying the spring constant and damping, as well as the value of the system peak is of paramount importance since by absorbing so much energy, this value of 75 % is linked to the establishment time and the energy that is has to stabilize the system. However, by having a lower vibration in the suspension system, it transmits greater kinetic energy to the body. Therefore, affecting the driving experience, so this type of suspension meets the optimal parameters for the correct power dissipation at right times [30].

This research requires the use of the CAD program like ANSYS 2020 for the corresponding simulation of the suspension system, incorporating

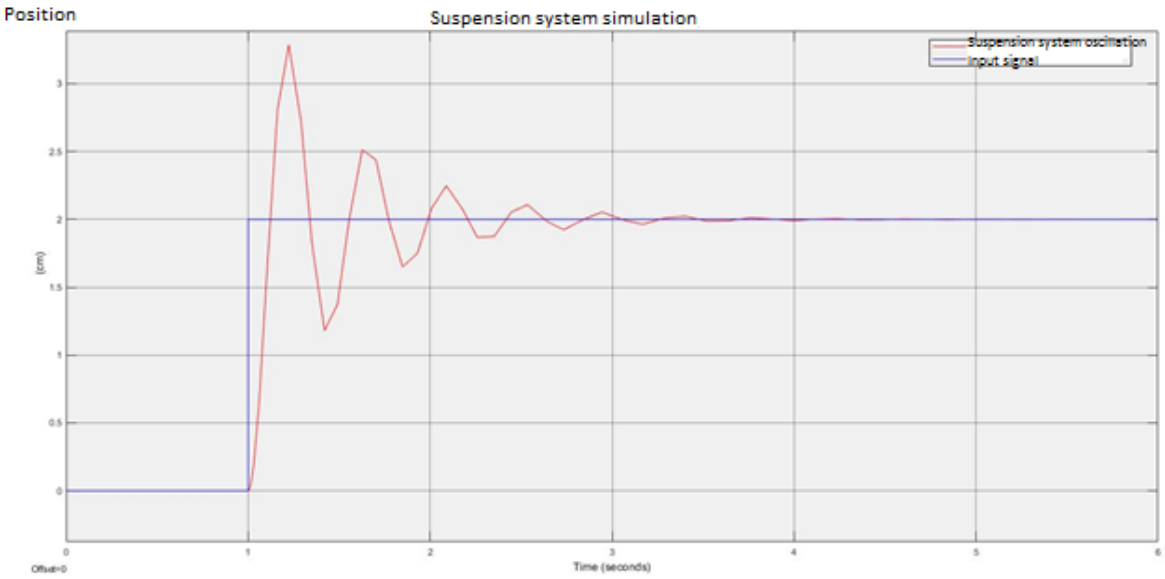

Figure 5: Suspension system oscillations under set parameters

the mesh of the suspension system and reaching the verification of the quality of the element through the mesh quality presentation offered by the ANSYS student community where a quality of the skewness metric parameter evidenced for 0,40063 which refers to a very good quality and an orthogonal quality parameter corresponding to 0,7329; significant of an equally very good quality as referred the theory evidenced below (Figure 6).

As stated above, we proceed to perform the test in which the system suspended has two rolling brackets and a maximum force, which was previously calculated at the top end of this, since it is the part that is fixed to the chassis of the vehicle and transmits the loads, Figure 7. Likewise, a mesh sizing is made which becomes thinner on the stem and spring of the damping since they are the areas of interest in deformation stresses.

By implementing the ANSYS 2020 R1 program, it is possible to generate a meshing of the suspension system with an applied force calculated in equation (12). Performing a rounding approximation of 7200 N and its due movement restrictions on the lower pin supports a stop. Having said the above, we proceed to a suspension system solution in which a focus is made on total deformation, the equivalent elastic deformation of von-Mises, and the equivalent effort of von-Mises Table 5. According to the data provided by this simulation, it is observed that the suspension stem suffers the highest efforts and elastic limits, so that it could result in future defects or discontinuities due to fatigue or external loads in this. Likewise, a focus is made on this last effort as it is the one that gives us the information necessary to have an understanding of the maximum value in MPa and understand if the material fails with respect to the properties said in Figure 8 for this suspension system with SAE 6150 H steel.

According to the data obtained in figure 8, a topological analysis study is carried out in order to obtain a reduction in efforts and to be able to opt for another type of shock which generates greater reliability in both performance parameters and compliance with the regulations of the regulations of Baja SAE Design. Having said that, this study is generated in such a way that the restrictions are assigned Figure 8. Optimization such as the bottom bracket and shock spring as you do not want to delete or reduce material from these areas as they would affect the operation of the system for malfunction (Figure 9) [31].

Skewness mesh metrics spectrum:

Excellent	Very good	Good	Acceptable	Bad	Unacceptable
0-0.25	0.25-0.50	0.50-0.80	0.80-0.94	0.95-0.97	0.98-1.00

Orthogonal Quality mesh metrics spectrum:

Unacceptable	Bad	Acceptable	Good	Very good	Excellent
0-0.001	0.001-0.14	0.15-0.20	0.20-0.69	0.70-0.95	0.95-1.00

Figure 6: ANSYS mesh quality

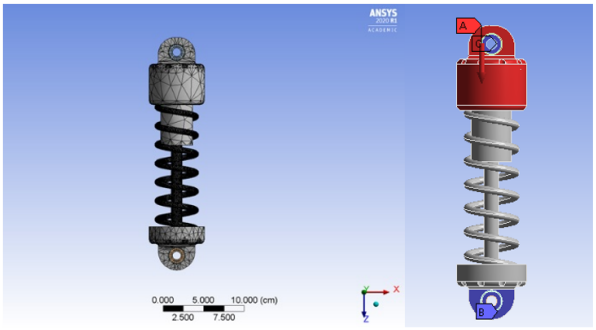

Figure 7: Meshing, Loads and structural supports applied to the suspension system

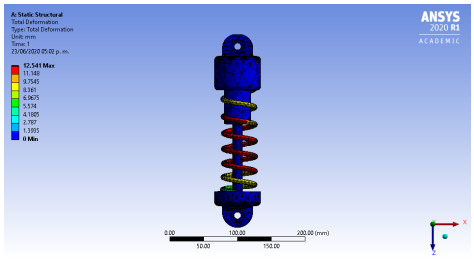

(a) Total deformation

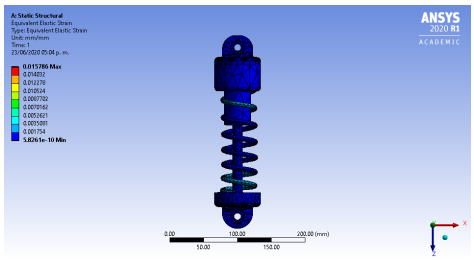

(b) vonVon-Mises equivalent elastic deformation

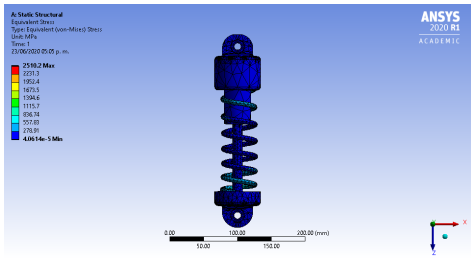

(c) vonVon-Mises' equivalent effort

Figure 8: Results for simulation in suspension system

Once optimization is implemented, it is observed that there are areas such as the lower head that can be reduced by positively affecting the system and evidence that an extension of the diameter can be generated in the stem head. For the above, modifications are made to the Cad SolidWorks so that the shank diameter is extended, the diameter of the shock is enlarged, and the size of the lower head is reduced as seen in Figure 10.

This variation in shock dimensions represents changes in maximum stress at the time of application of the same 7200 N load provided in the kinematic study of the maximum load received by the shock in a given instant of time. In this way a second static load study is carried out using the CAD program ANSYS 2020R1 in which variations are observed in terms of all stress values and deformations, resulting in a 5,34% decrease in the shock mass and reduction an equivalent effort being now 662,42 MPa. According to the properties of the material SAE 6150 H in Table 4. Its elastic limit

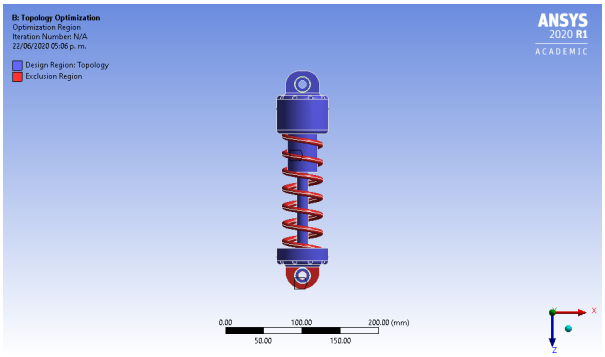

Figure 9: Areas to exclude in topological optimization

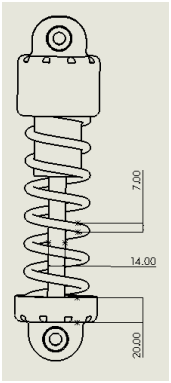

(a) Shock absorber JLMotor 250mm without topologically optimizing (mm)

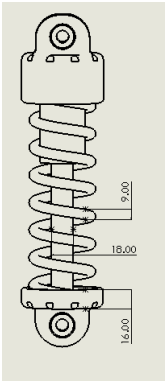

(b) Topologically optimized JLMotor 250mm shock absorber (mm)

Figure 10: JLMotor 250 mm buffer design modifications

is 800 MPa which represents that such topological study and modification of the suspension geometry helps to reduce the failure in the elastic area of the material that could occur when having irregularities of the terrain. The implementation of the topological study helps reduce the efforts and deformations as seen in Table 7. This way it can be selected under the JLMotor catalogs the type of suspension with the same or similar design characteristics proposed and thus is more optimally adapted due to the external parameters and factors posed by the SAE [32, 33, 20].

Table 7: Stress and deformation values for JLMotor 250 mm shock before and after topological optimization

	JLMotor 250mm shock absorber	JLMotor 250mm shock absorber topologically optimized
Mesh (mm)	300	300
Sizing (mm)	2	2
Elements	15168	15780
Nodes	31129	31506
Skewness	0,40063	0,46614
orthogonality quality	0,7329	0,7329
Element quality	0,66375	0,59083
Total deformation (mm)	12,541	52,578
Equivalent elastic deformation (mm / mm)	0,00011672	0,000381
Equivalent stress (MPa)	2510,2	662,41
Mass (kg)	25,984	24,595

According to the data provided by the simulations regarding the optimizations of the topological and performance of this in when the static simulation, the purchase of the shock absorber shock JLMotor 3100026 (Figure 11).

5. Discussions

Analyzing the results of total deformation, elastic deformation equivalent of von-Mises and effort equivalent of von-Mises obtained with a mesh of 350 mm and topological optimization to avoid defects due to external loads in steel 6150 H, together with design considerations such as topological optimization, three important points can be highlighted of the results obtained:

1. The selected suspension system from the JLMoto catalog meets the design and SAE

Source: Jl motor official store. https://bit.ly/3p66Gxi

Figure 11: JLMoto brand suspension system dimensioning reference 3100026

requirements for optimal competitive operation with the consideration that said simulated model does not respond to machining cost issues in its topological optimization and vibration reduction without affecting the mechanical properties of the material.

2. An equivalent Von-Mises stress value is achieved by ANSYS 2020R1 of 662,41 MPa, thus ensuring that the suspension system does not fail under the critical conditions of dynamic displacement, because the elastic limit of the SAE 6150 H material is 800 MPa.

3. The ANSYS software through the topological study allows reducing the shock mass by 5,34 %; making it lighter and with better performance mechanical characteristics for the conditions posed by the SAE formula and making a contribution to the automotive industry from the mechanical Engineering.

6. Conclusions

The topological optimization of the suspension system can contribute to the automotive sector at the same time reducing costs in materials and manufacturing times. In this way, it is advisable to evaluate the conditions to which the suspension system will be exposed, and accordingly, areas that do not have stress concentrators are optimized.

The analysis of oscillations over time shows a high overshoot and an establishment in four seconds, for which the system adequately absorbs the irregularities of the ground without suffering high efforts that compromise the material and generate discontinuities or cracks.

The suspension system designed exclusively for competition provides greater reliability and improved results in terms of time reduction and absorption of terrain irregularities, providing comfort and a pleasant driving experience.

7. Acknowledge

To the Research Center of the Faculty of Engineering of the Universidad Libre, headquarters in Bogotá for carrying out the financing of the research project “Design and manufacture of low mini vehicle V.1.0 under SAE parameters”, which has allowed the SIM Semillero and its members to make presentations and articles at scientific events, which has strengthened the competitions in the maintenance line for students of the Mechanical Engineering Program.

8. References

[1] G. I. Y. Mustafa, H. P. Wang, and Y. Tian, “Vibration control of an active vehicle suspension systems using optimized model-free fuzzy logic controller based

on time delay estimation," *Advances in Engineering Software*, vol. 127, pp. 141–149, 2019.

[2] J. A. García-Manrique, S. Peña-Miñano, and M. Rivas, "Manufacturing to motorsport by students," *Procedia Engineering*, vol. 132, pp. 259–266, 2015.

[3] S. Chepkasov, G. Markin, and A. Akulova, "Suspension kinematics study of the "Formula SAE" sports car," *Procedia Engineering*, vol. 150, pp. 1280–1286, 2016.

[4] R. Burdzik, "Novel method for research on exposure to nonlinear vibration transferred by suspension of vehicle," *International Journal of Non-Linear Mechanics*, vol. 91, pp. 170–180, 2017.

[5] I. V. Ryabov, V. V. Novikov, and A. V. Pozdeev, "Efficiency of shock absorb in vehicle suspension," *Procedia Engineering*, vol. 150, pp. 354–362, 2016.

[6] G. M. Szyma-ski, M. Josko, F. Tomaszewski, and R. Filipiak, "Application of time–frequency analysis to the evaluation of the condition of car suspension," *Mechanical Systems and Signal Processing*, vol. 58–59, pp. 298–307, 2015.

[7] E. Sert and P. Boyraz, "Optimization of suspension system and sensitivity analysis for improvement of stability in a midsize heavy vehicle," *Engineering Science and Technology, an International Journal*, vol. 20, no. 3, pp. 997–1012, 2017.

[8] B. Németh and P. Gáspár, "LPV-based Variable-Geometry Suspension Control Considering Nonlinear Tyre Characteristics," *IFAC-PapersOnLine*, vol. 48, no. 26, pp. 61–66, 2015.

[9] C. Kavitha, S. A. Shankar, K. Karthika, B. Ashok, and S. D. Ashok, "Active camber and toe control strategy for the double wishbone suspension system," *Journal of King Saud University - Engineering Sciences*, vol. 31, no. 4, pp. 375–384, 2018.

[10] J. Díaz-Mendoza, L. Vidal-Portilla, C. Ramírez-Espinoza, y C. González-Pinzón, *Diseño de un vehículo Baja SAE*, ser. Colección Textos Universitarios. Serie Investigación. Universidad Autónoma de Ciudad Juarez, 2013.

[11] S. K. Sharma, V. Pare, M. Chouksey, and B. R. Rawal, "Numerical studies using full car model for combined primary and cabin suspension," *Procedia Technology*, vol. 23, pp. 171–178, 2016.

[12] M. Nagarkar, Y. Bhalerao, G. Patil, and R. Patil, "Multi-Objective Optimization of Nonlinear Quarter Car Suspension System – PID and LQR Control," *Procedia Manufacturing*, vol. 20, pp. 420–427, 2018.

[13] H. Jing, R. Wang, C. Li, and J. Bao, "Robust finite-frequency H. control of fullcar active suspension," *Journal of Sound and Vibration*, vol. 441, pp. 221–239, 2019.

[14] H. Carlson, *Spring Designer's Handbook*. CRC Press, 1978.

[15] S. Saurabh, K. Kumar, S. Kamal-Jain, S. Kumar-Behera, D. Gandhi, S. Raghavendra, and K. Kalita, "Design of suspension system for formula student race car," *Procedia Engineering*, vol. 144, pp. 1138–1149, 2016.

[16] G. Shelke, A. Mitra, and V. Varude, "Validation of Simulation and Analytical Model of Nonlinear Passive Vehicle Suspension System for Quarter Car," *Today Materials: Proceedings*, vol. 5, no. 9, pp. 19 294–19 302, 2018.

[17] W. Wang and Y. Song, "Analytical computation method for steady-state stochastic response of a time-delay nonlinear automotive suspension system," *Mechanical Systems and Signal Processing*, vol. 131, pp. 434–445, 2019.

[18] A. Keivan and B. Phillips, "Rate-independent linear damping in vehicle suspension systems," *Journal of Sound and Vibration*, vol. 431, pp. 405–421, 2018.

[19] G. Yan, M. Fang, and J. Xu, "Analysis and experiment of time-delayed optimal control for vehicle suspension system." *Journal of Sound and Vibration*, vol. 446, pp. 144–158, 2019.

[20] Associated Spring-Barnes Group, *Design Handbook*. Bristol, Conn, 1987.

[21] D. Pastorcic, G. Vukelic, and Z. Bozic, "Coil spring failure and fatigue analysis," *Engineering Failure Analysis*, vol. 99, pp. 310–318, 2019.

[22] Y. Mohammad-Hashemi, M. Kadkhodaei, and M. Mohammadzadeh, "Fatigue analysis of shape memory alloy helical springs," *International Journal of Mechanical Sciences*, vol. 161–162, p. 105059, 2019.

[23] T. Keerthi vasan, S. Shibi, and C. Tamilselvan, "Fabrication and testing of composite leaf spring using carbon, glass and aramid fiber." *Materials Today: Proceedings*, vol. 21, pp. 45–51, 2019.

[24] J. Foard, D. Rollason, A. Thite, and C. Bell, "Polymer composite belleville springs for an automotive application." *Composite Structures*, vol. 221, p. 110891, 2019.

[25] X. Ma, P. Wong, and J. Zhao, "Practical multi-objective control for automotive semi-active suspension system with nonlinear hydraulic adjustable damper," *Mechanical Systems and Signal Processing*, vol. 117, pp. 667–688, 2019.

[26] M. Omar, M. El-kassaby, and W. Abdelghaffar, "Parametric numerical study of electrohydraulic active suspension performance against passive suspension," *Alexandria Engineering Journal*, vol. 57, no. 4, p. 36093614, 2018.

[27] M. Benko, L. Kucera, and L. Smetánka, "Front suspension design of the lightweight vehicle," *Transportation Research Procedia*, vol. 40, pp. 623–630, 2019.

[28] A. Furg, A. Myrell, A. Killinger, and R. Gadow, "Suspension and coating characterization of high velocity suspension flame sprayed (HVSFS) mixed titanium oxide–titanium carbide coatings," *Surface and Coatings Technology*, vol. 371, pp. 90–96, 2019.

[29] J. Shigley and C. Mischke, *Design in Mechanical*

Engineering, 6th ed. Mexico: McGrawHill, 2002.

[30] L. Harus and H. Wiwiek, "A Comparative Study of the Damping Force and Energy Absorbtion Capacity of Regenerative and Conventional-Viscous Shock Absorber of Vehicle Suspension," *Applied Mechanics and Materials*, vol. 758, pp. 45–50, 2015.

[31] J. Rumney, "Construction of motor vehicle springs," *Transactions (Society of Automobile Engineers)*, vol. 2, no. 2, pp. 45–56, 1907.

[32] C. Patiño, C. Calderon, J. Ortiz, y O. Rodríguez, "Diseño y construcción de un prototipo mini baja SAE," Trabajo para optar al título de Ingeniero Mecánico, Universidad Pontificia Bolivariana., Bucaramanga, 2008.

[33] V. Chacón, "Diseño de una suspensión para un vehículo automóvil basada en amortigaudores magneto-reológicos," Trabajo para optar a la título de Ingeniería Técnica Industrial, Especialidad Mecánica, Escuela Politécnica Suerior de la Universidad Carlos III de Madrid, 2009.